Clay Minerals (1988) **23**, 423–437

HALLOYSITE FORMATION THROUGH *IN SITU* WEATHERING OF VOLCANIC GLASS FROM TRACHYTIC PUMICES, VICO'S VOLCANO, ITALY

P. QUANTIN, J. GAUTHEYROU AND P. LORENZONI*

*ORSTOM, 70 route d'Aulnay, 93143 Bondy Cedex, France, and *ISSDS, Piazza d'Azeglio 30, Firenze, Italy*

(*Received October 1987; revised 5 April 1988*)

ABSTRACT: The weathering of a trachytic pumice within a pyroclastic flow underlying an andic-brown soil on the volcano Vico has been studied. The main mineral formed is a spherical 10 Å halloysite which has been shown by SEM and *in situ* microprobe analysis to have formed directly from the glass. The major mineralogical characteristics as determined by XRD, IR, DTA, TEM and microdiffraction are typical of 10 Å halloysite. However, some minor mineralogical properties and the high Fe and K contents, suggest that it is an interstratification of 74% halloysite and 26% illite-smectite. The calculated formula of the hypothetical 2:1 minerals reveals an Fe- and K-rich clay, with high tetrahedral substitution, like an Fe-rich vermiculite, but the detailed structure of this mineral remains uncertain.

This study deals with the weathering of trachytic pumices to a white clay which seems to be derived directly from glass, without change in texture. This clay is a well crystallized 10 Å halloysite, and although nearly white in colour, has an unusual composition being rich in Fe and Ti, and having a high K content. The aims of the study are to show the transformation of glass into halloysite, to discuss the structural formula of this clay mineral, and to suggest the hypothesis of a composite building of 1:1/2:1 phyllosilicates.

MATERIALS AND METHODS

The weathering of trachytic pumices has been observed in the fourth pyroclastic flow of Vico, in the Latium, Italy (Fig. 1). This flow dates back to about 140,000 BP (Sollevanti, 1983) and is covered by an andic-brown soil (andic Dystrochrept) under which the coarse pumices are almost completely weathered to a white gel whereas the flow matrix is weakly altered. As the alteration occurs only at the top of the flow, near the soil, it is probably due to weathering. The reference soil profile, related to the weathered pumice sample, is Vico 29 (Lorenzoni *et al.*, 1986; Bidini *et al.*, 1987). An unaltered pumice from the bottom of the flow, and a strongly weathered pumice from the top, near the soil, have been analysed. The petrography of the unaltered pumice was studied in thin section by optical microscopy. The mineralogy of the powdered rock was determined by X-ray diffraction (XRD) and the chemical composition was obtained by a Li metaborate fusion method.

The weathered pumice was studied *in situ* along a transect (Fig. 2), from the weakly weathered greyish core, through a semi-altered transition zone, to the completely weathered white cortex, first by optical microscopy, and then by scanning electron microscopy (SEM)

© 1988 The Mineralogical Society

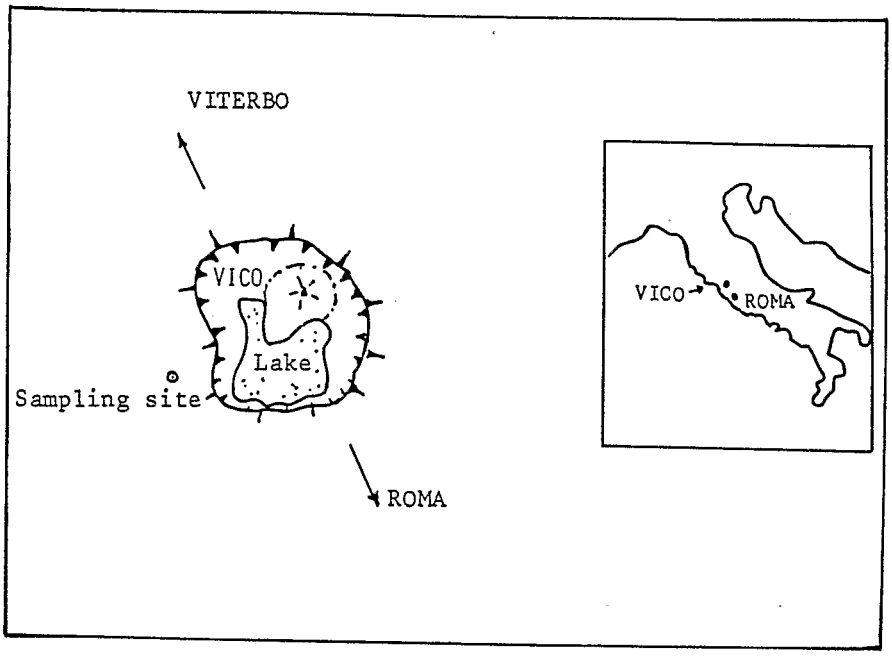

FIG. 1. Location of Vico's volcano.

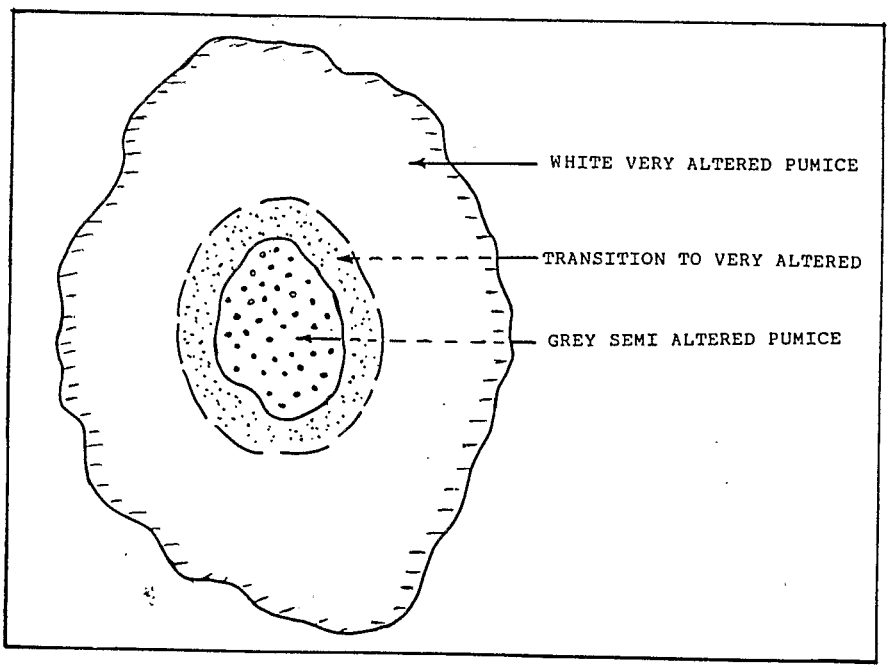

FIG. 2. Transect across altered pumice.

and microprobe analysis for the major elements. The $< 2\ \mu m$ fraction was separated from the powdered rock after cation exchange with NH_4^+ and dispersion by ultrasonic agitation, and the $< 0{\cdot}2\ \mu m$ fraction further separated by ultracentrifugation.

XRD was performed on the whole powder, on the $> 2\ \mu m$ fraction (wet, and also dehydrated at 100°C) and on the oriented $< 2\ \mu m$ fraction (wet, glycerol solvated, dehydrated at 100°C, and calcined at 470°C). The $< 2\ \mu m$ fraction was also studied by transmission electron microscopy (TEM), infrared spectroscopy (IR), (on the sample wet, and dehydrated at 100°C and 180°C), differential thermal analysis (DTA) and thermo gravimetric analysis (TGA). The $< 0{\cdot}2\ \mu m$ fraction was examined by TEM. Chemical analysis of the major elements were obtained on the "triacid" extract of the whole weathered pumice powder (ORSTOM Laboratory of Chemistry method), and by microprobe analysis on the $< 2\ \mu m$ fraction. The cation exchange capacity (CEC) of the whole powder was determined at pH 4 and pH 7 by NH_4 oxalate-oxalic acid extraction (Quantin, 1982), and allophane and paracrystalline oxides were determined by the NH_4 oxalate (pH 3, in the dark) method (Parfitt & Henmi, 1982).

THE WEATHERING CONDITIONS

The ambient climate is near to wet-temperate (Lulli *et al.*, 1988) with an annual rainfall of ~ 1400 mm. The weathering of pumices is due to the slow infiltration of rainwater from the soil through the weakly-permeable matrix of the volcanic tuff. However, there is not any obvious illuviation of humic acids or mineral products from the soil. The soaked white pumices are very weathered and very hydrated ($H_2O^- = 65\%$) whereas, around the pumices, the cement matrix and the fragments of massive lava remain weakly altered. This rapid alteration of the pumice is due to its high porosity as well as to the fibrous texture of the glasses. There has not been any alteration prior to pedogenesis as occurred with the "argillified" pyroclastic tuffs of Mt. Sabatini, near Bracciano in Italy (Lenzi & Mattias, 1978). The poor permeability of the tuff results in a waterlogged environment with very slow vertical drainage. At the base of the soil, the weathered tuff (ref. samples 29C and 29R1, Bidini *et al.*, 1987) has a pH of 7·2, and a CEC of 70 mEq/100 g composed of 40 mEq/100 g Ca^{2+}, 24 mEq/100 g K^+ and 4 mEq/100 g Mg^{2+}. However, the weathered pumice under the soil has a pH of 6·2, revealing a slight cation-lixiviation in the pumice itself.

RESULTS

The grey unaltered pumice

The pumice is composed of hair-like vesicular glass ($> 80\%$) and crystals of sanidine, green augite, biotite and titano-magnetite, as well as a few relics of zeolitized leucite (Table 1). The chemical composition is similar to that of an alumina-rich alkaline-potassic trachyte ($Al_2O_3 = 24\%$, $K_2O = 7{\cdot}1\%$, $Na_2O = 2{\cdot}6\%$) poor in Fe, Ti, Mg and Ca (Table 2).

The white weathered pumice

In situ observations. When examined by optical microscopy, the pumice is seen to retain its original fibrous vesicular texture, even in the completely weathered white cortex (Fig. 3a).

TABLE 1. Mineralogical composition.

Grey Pumice[1]		White Pumice[2]		
		Fraction	>2 μm	<2 μm
Glass	++++	10 Å Halloysite	++++	8
Sanidine	++	Mica; 10–14 Sm	++	1
Augite	+	Zeolites	+	<0·5
Biotite	+	Sanidine	++	—
Ti-Magnetite	+	Augite	+	—
Zeolites	tr	Ti-Magnetite	+	<0·5

[1]Grey = very weakly altered; [2]White = strongly altered.
++++ >60%; ++ 10–20%; + 5–10%; tr trace.

TABLE 2. Chemical composition.

Oxides normalised %	Whole unaltered pumice (1)	*in situ* microprobe analysis: grey core (2)	→ transition ring (2)	→ white a (2)	cortex b (2)	Whole altered pumice (3)	White <2 μm fraction (4)
SiO_2	57·79	56·81	52·29	51·63	49·94	49·66	50·84
Al_2O_3	24·26	34·48	35·89	38·18	38·40	37·58	38·62
Fe_2O_3	3·88	3·99	6·07	6·57	7·03	7·30	7·25
TiO_2	0·52	0·64	0·84	0·84	0·84	0·98	1·00
MnO	0·15	0·06	0·00	0·06	0·00	0·07	0·13
MgO	0·68	0·22	0·24	0·24	0·30	0·49	0·29
CaO	2·88	0·88	1·18	0·78	0·62	1·76	0·66
K_2O	7·12	2·07	2·17	1·36	1·67	1·69	0·97
Na_2O	2·59	0·32	0·28	0·17	0·28	0·29	0·01
P_2O_5	0·10	0·22	0·14	0·18	0·19	0·15	0·22
SO_3	n.d.	0·30	0·87	—	0·74	—	—
Mol. SiO_2/Al_2O_3	4·05	2·80	2·48	2·30	2·21	2·24	2·24
Mol. SiO_2/R_2O_3	3·67	2·61	2·24	2·07	1·99	1·99	2·00

(1) Whole pumice, by fusion method; (2) by microprobe: a—windows at the surface of fibres, and b—spots on single particles; (3) whole white pumice, by "Tri-acid extraction"; (4) <2 μm powder, by microprobe.

Phenocrysts of sanidine, augite, biotite and magnetite remain unaltered and some very small opaque crystals of magnetite can be seen along the fibres. There is no product of illuviation.

The fibrous texture can also be seen by SEM in its original form in the core as well as in the cortex (Fig. 3b), but the glass surface looks more granular in the white cortex than in the grey core (Fig. 3c). At higher magnification, the completely weathered glass shows sub-angular or rounded grains on the surface (Fig. 3c) and a parallel stacking of small plates ~1 μm in size (Fig. 3d), which seem to be a clay weathering product of the glass.

Microprobe analyses were made *in situ* on the glass surface and on the fibrous section on the scale of a single grain (1 μm^2). The average values of the analyses on the glass surface show a chemical evolution from the core to the cortex (Table 2). This progression results from

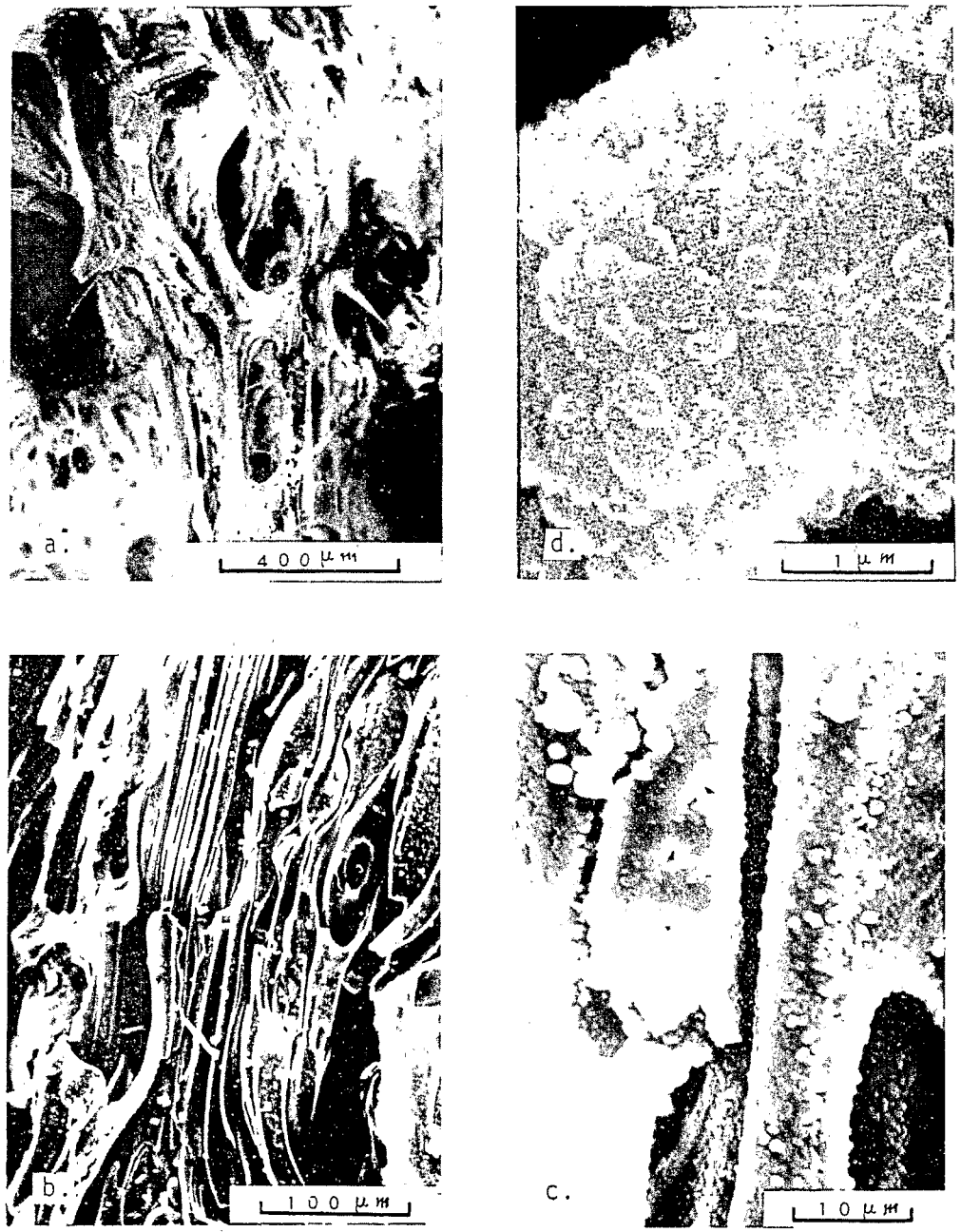

FIG. 3. Microscopy of altered pumice fragment. (a) Fibrous texture and Ti-magnetite grains as observed by optical microscopy. SEM photomicrographs of (b) general view of altered fibres, (c) detail on fibre surface, (d) stacking of clay particles.

the variation of molecular SiO_2/Al_2O_3 and SiO_2/R_2O_3 ratios from 2·8 to 2·2, and from 2·6 to 2·0, respectively. Comparison with the unaltered pumice shows a decrease in Si, Mg, Ca, K and Na, and a large increase in the more stable elements such as Al, Fe and Ti. However, the decrease in Si seems small, and the K content remains considerable (1·7–1·0% K_2O).

The spot analysis of single grains in the section of completely altered fibres shows an almost constant chemical composition (Table 2), namely, mol. $SiO_2/Al_2O_3 = 2·2$, mol. $SiO_2/R_2O_3 = 2·0$, $K_2O = 1·7\%$, $Fe_2O_3 = 7\%$, $TiO_2 = 0·8\%$, $MgO = 0·3\%$ and $CaO = 0·6\%$. This composition is constant at the grain scale (1 μm^2) as well as on small homogeneous surfaces ($\simeq 200$ μm^2 area). This rules out the possibility of a mixture of clay minerals and some relics of primary minerals (> 1 μm in size).

Analysis of the weathering products. The weathered pumice is composed mainly of a well-crystallized 10 Å halloysite, the very intense and sharp peak at 10 Å collapsing to 7·15 Å after dehydration at 100°C (Fig. 4). Residual primary minerals are more obvious on the XRD trace of the > 2 μm fraction and include biotite, sanidine, augite and zeolites (phillipsite peak at 5·6 Å). These minerals, as well as titano-magnetite, have also been identified by optical microscopy and microprobe analysis.

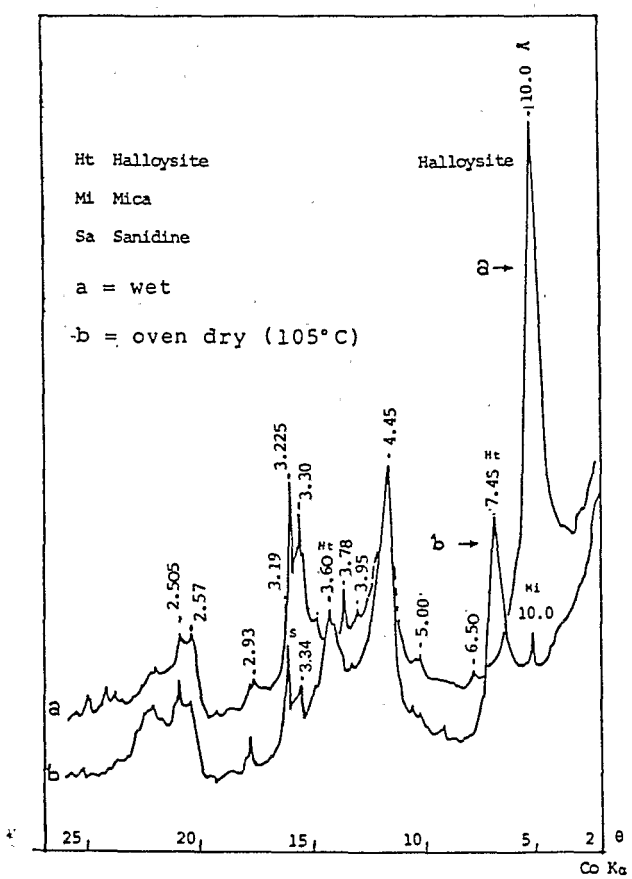

FIG. 4. XRD patterns of whole altered pumice.

The XRD traces of the <2 μm fraction (Fig. 5) are typical of a well-crystallized, hydrated halloysite with peaks at 10·0, 4·45, 3·34 and 2·555 Å when wet, 7·5–7·3 and 3·56 Å after dehydration at 100°C, and 10·6 and 3·65 Å after glycerol solvation (Fig. 5). Furthermore, the peak at 7 Å disappears after calcination at 470°C. Very weak reflections are apparent near 10, 12 and 14 Å after dehydration at 100°C, there is some swelling to 16 and 20 Å after glycerol solvation, and some weak reflections persist near 10·2, 4·49, 3·34 and 2·44 Å after dehydroxylation of the halloysite at 470°C. It seems, therefore, that there is some expandable 10–14 Å clay mineral which could be an irregular interstratified mineral of illite-smectite type. There is no clear evidence for the presence of iron oxide or any other mineral.

The IR spectrum of the <2 μm fraction (Fig. 6) is consistent with hydrated halloysite, particularly the bands of OH vibrations near 3700 and 3620 cm^{-1}. However a broad band between 3600 and 3150 cm^{-1} is still present after dehydration at 180°C (Fig. 6b) and could be related to the OH vibration of a 2:1 clay mineral. A small sharp band at 1400 cm^{-1} could indicate NH_4^+ adsorption by the clay (Bartoli, personal communication). In addition, a weak shoulder near 880 cm^{-1} on the 910 cm^{-1} band of halloysite is related to the stretching vibration of OH linked to the octahedral Fe(III)–Al couple in Fe-rich smectites (Farmer,

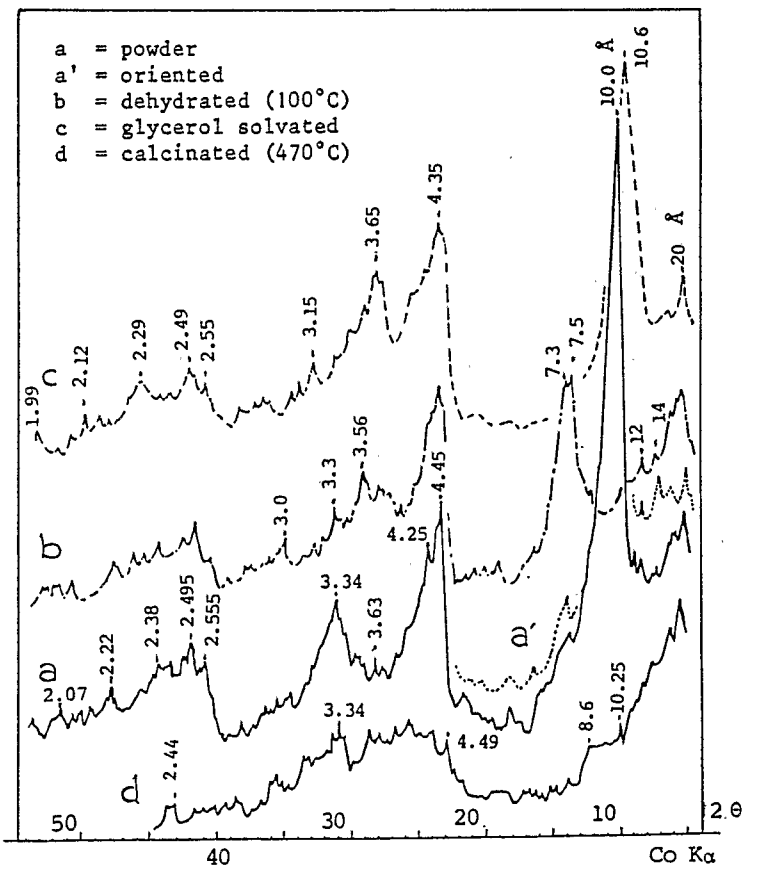

FIG. 5. XRD patterns of <2 μm fraction.

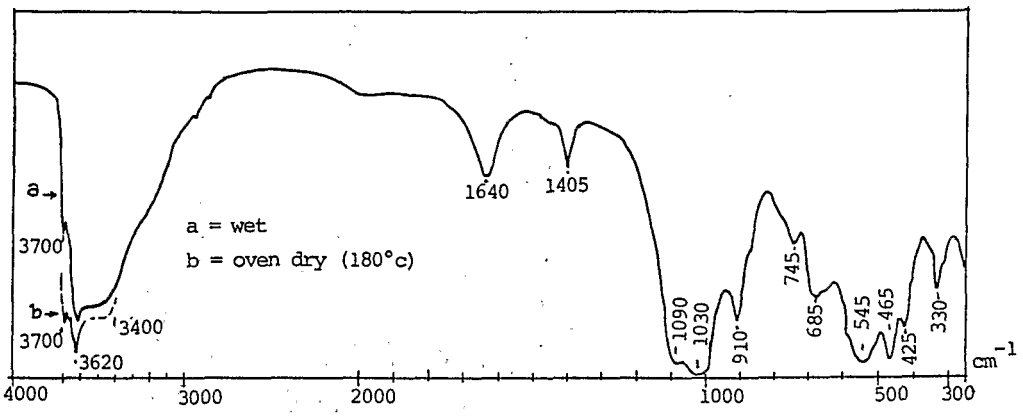

FIG. 6. IR spectrum of <2 μm fraction.

1974; Goodman *et al.*, 1976), as well as in Fe-rich halloysites (Kunze & Bradley, 1964; Wada & Mizota, 1982; Quantin *et al.*, 1984).

TEM reveals many spherical shapes of halloysite with diameter 10–100 nm (Fig. 7a,b). The smallest are probably transitional between allophane and halloysite. There are also some crumpled or somewhat rolled, lamellar clays (Fig. 7d), which look like beidellite or could be an interstratified halloysite-hisingerite mineral (Quantin *et al.*, 1984) or an Fe-rich halloysite (Tazaki, 1982). There are a few broken flakes of mica due to the disintegration of biotite during the clay extraction. In addition, some very small opaque discs (diameter 1–10 nm) can be observed around or inside some spherical halloysite (Fig. 7c, d) which could be mostly opal (Shoji & Masui, 1971; Quantin & Rambaud, 1987) or iron oxide.

Microdiffraction of spherical shapes of halloysite by TEM shows 3 rings of high intensity near 4·44, 2·255 and 1·485 Å, which are the main (020), (130) and (060) reflections of a dioctahedral clay. In addition, there are weak or very weak diffraction rings near 4·6, 4·36, 2·72, 1·74, 1·69, 1·54, 1·38, 1·33, 1·29 and 1·25 Å, most of which correspond to the reticular distances of halloysite. But the very weak reflections near 4·6, 1·74 and 1·54 Å suggest a few Fe-rich clay minerals (illite, hisingerite, nontronite).

The DTA curve (Fig. 8) is typical of that for a hydrated halloysite, with two endothermic reactions at 135 and 515°C, as well as a sharp exothermic peak at 865°C. Compared to the curve for a well crystallized kaolinite (Macon, Georgia), there is an increase in the 135°C peak (dehydration), the dehydroxylation peak occurs at 515°C rather than 560°C, and the exothermic peak occurs at 865°C rather than 920°C. However, the curve for the whole altered pumice shows very weak endothermic reactions near 580°, 675°, 820° and 850°C, which could indicate the presence of a little biotite (as observed in the >2 μm fraction) and smectite. From TGA (Fig. 9), the weight loss of the <2 μm hydrated clay from 25° to 1025°C is 22·31% composed of 12·31% H_2O^- from 25°C to 250°C (8·46% from 25° to 105°C, and 3·85% from 105° to 250°C), and 10·00% H_2O^+. In fact, the weight loss due to dehydroxylation amounts to 11·40% relative to anhydrous clay (at 250°C), which compared to 13·7%, the theoretical weight loss of anhydrous kaolinite (Caillere & Henin, 1963), means there could only be 83·2% kaolinite in the sample studied. But if we consider a mixture of 1:1 and 2:1 clay minerals, as suggested by DTA, the proportion of the two components can be calculated on the basis of a theoretical weight loss of 5% (anhydrous clay at 250°C) for the 2:1 clay mineral, resulting in ~74% kaolinite and 26% 2:1 clay mineral.

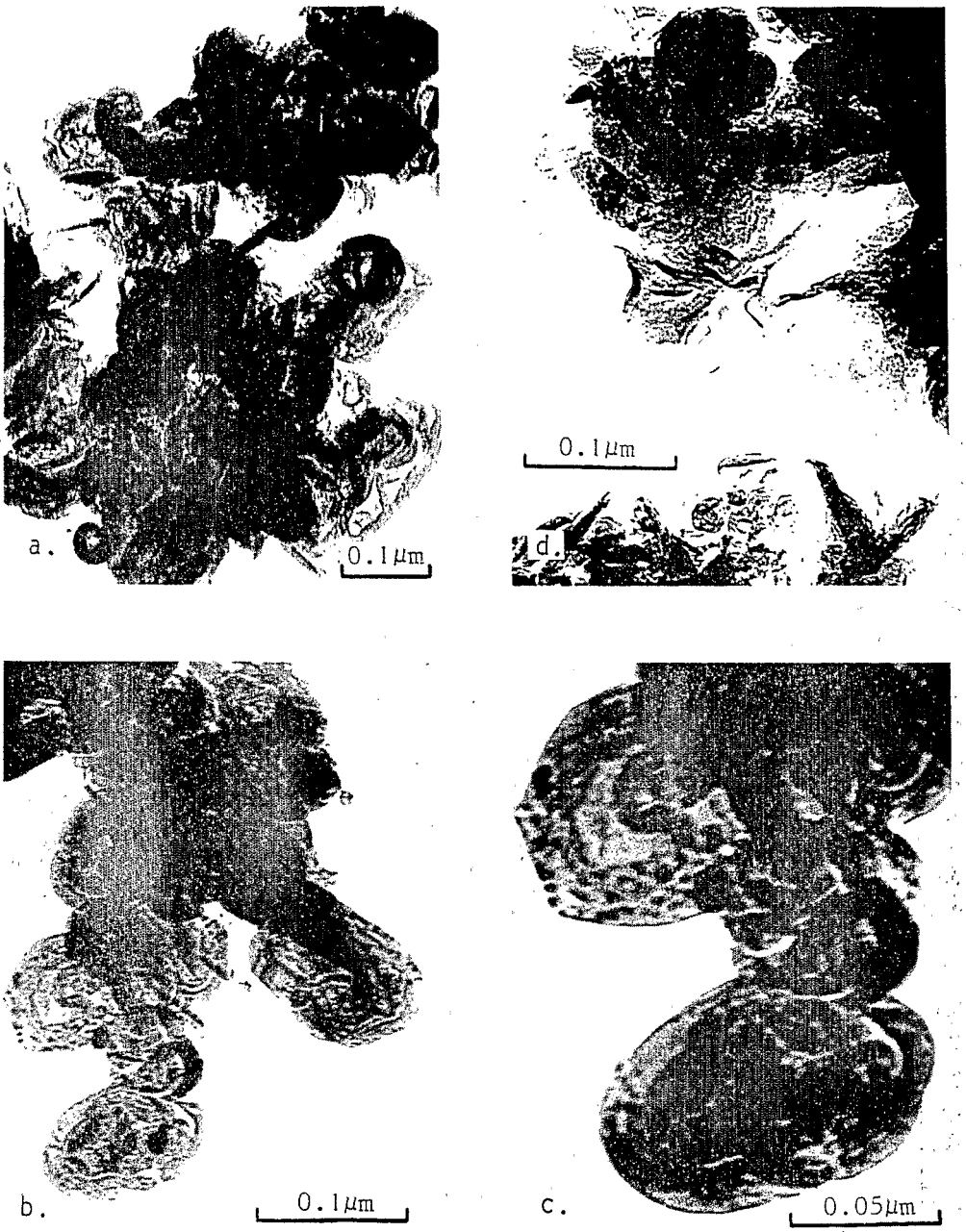

FIG. 7. TEM of <2 μm fraction. (a, b) spherical halloysite; (c) detail on spherical halloysite, note small opaque discs; (d) spherical and crumpled lamellar clays.

The "triacid" extract of the whole material includes the whole weathering product as well as Ti-magnetite and zeolites, but not the other primary minerals which are insoluble. The analyses (Table 2) have been normalized to 100% of the anhydrous product. It is worth noting that the results (except CaO) are very close to the average values obtained by the *in situ*

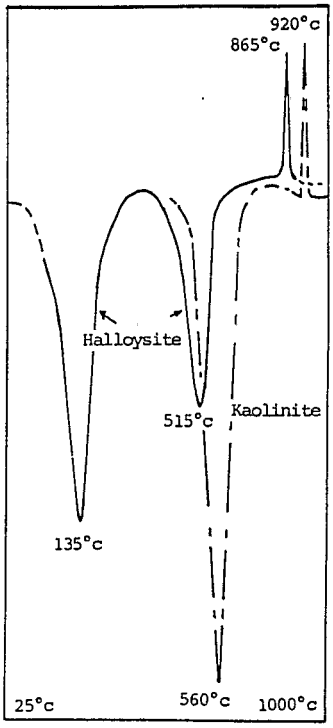

FIG. 8. DTA curve of <2 μm fraction.

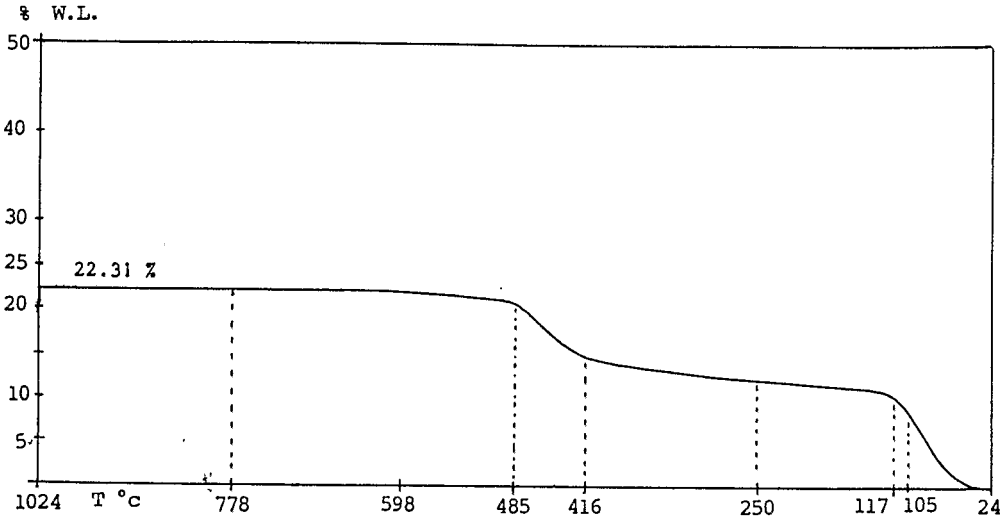

FIG. 9. TGA curve of <2 μm fraction.

microprobe analysis on the glass surface, in the completely weathered cortex. The microprobe analysis of the <2 μm fraction is similar to those on the pumice at the window scale (200 μm^2) as well as on a spot (1 μm^2) except that the K_2O content is lower, 1% instead of 1·7%. This is probably due to K^+ exchange by NH_4^+ during the clay pretreatment. The molecular ratios SiO_2/Al_2O_3 (2·2) and SiO_2/R_2O_3 (2·0) are also similar. The CEC of the whole weathering product is 65·6 mEq/100 g at pH 7 and 58·8 mEq/100 g at pH 4. The content of exchangeable cations is 29·31 mEq/100 g K^+, 17·62 mEq/100 g Ca^{2+}, 5·07 mEq/100 g Na^+ and 4·63 mEq/100 g Mg^{2+} (based on the clay content at 105°C). The base saturation ratio is 86·4% at pH 7 and 96·3% at pH 4 indicating that the permanent CEC of the clay is ~58 mEq/100 g. The pH of 6·2 confirms a slight cation lixiviation in the weathered pumice. The NH_4 oxalate extraction gave the following results, in % clay content (at 105°C): $SiO_2 = 0·22$, $Al_2O_3 = 0·75$, $Fe_2O_3 = 0·12$, $K_2O = 1·27$, $MgO = 0·11$, $CaO = 0·01$. These data indicate that only traces of allophane and paracrystalline Al, Fe oxides are present. The allophane content could be either 0·72% on the basis of the imogolite formula (Si/Al = 0·5), or 0·47% on the basis of the kaolinite formula (Si/Al = 1), the corresponding free Al oxide content being 0·37% and 0·56%, respectively. The large amount of oxalate extractable K is almost equivalent to the exchangeable K^+.

INTERPRETATION

In situ observation of the weathering process

Microscopy shows that weathering is progressive from the cortex to the core of the pumice, and from the surface to the centre of the glass fibres. The weathering process is so rapid that phenocrysts of augite, biotite, sanidine and magnetite remain intact but the glass is transformed without change in the fibrous texture into the clay weathering product which forms small grains ~1 μm in size.

The *in situ* microprobe analysis (Table 2) reveals a classical process of weathering. The semi-altered core of the pumice contains more Si and K, and less Al, Fe and Ti than the completely altered white cortex. The chemical composition in the cortex has reached an almost constant limit at the scale of each elementary grain (diameter $\simeq 1$ μm). This shows that there is a high lixiviation of bases, and to a lesser extent of silica, out of the glass and a proportional concentration of metal oxides in the glass. However, the concentration is greater for Fe and Ti than for Al oxides, suggesting some leaching of Al. Fe and Ti oxides remain in the same ratio, about 7:1 but this ratio is half that in the Ti-magnetite crystals in the same pumice (14:1, by microprobe analysis), indicating that Ti could also be located in the silicates. The nearly white colour of the weathering product, although it contains 7% Fe_2O_3 and a very small amount of oxalate extractable Fe, shows that only a trace of Fe-oxyhydroxide was formed. The molecular ratios of $SiO_2/Al_2O_3 = 2·2$ and $SiO_2/R_2O_3 = 2·0$ suggest that the white weathering product is an Fe-rich aluminosilicate. Sodium is the most lixiviated of all the basic elements, but an important amount of Ca, Mg and especially K remains, probably retained by clay minerals.

Determination of the composition of the weathering product

The mineralogy of the <2 μm fraction has shown that a spherical 10 Å halloysite is the principal constituent. The clay contains ~7% Fe_2O_3, 1% TiO_2 and at least 1% K_2O

(anhydrous weight) and microprobe analysis indicates that it is homogeneous. From the SiO_2/Al_2O_3 and SiO_2/R_2O_3 ratios (2·2 and 2·0) it should be considered as an Fe-rich halloysite. Such an interpretation was proposed for similar clays by Kunze & Bradley (1964) and Weaver & Pollard (1973), and for a ferri-halloysite from Italy by Bonatti & Galitelli (1950) and Wada & Mizota (1982). However, for a similar "white iron-rich halloysite" (Quantin *et al.*, 1984) an interstratified halloysite-hisingerite mineral was postulated in order to take account of some mineralogical and physico-chemical properties of this clay. Delvaux *et al.* (1987) refer to this hypothesis for Fe-rich halloysite in soils derived from basaltic ash in the Cameroons.

Some minor peculiarities in the mineralogical properties of the clay show that it is not a pure dioctahedral 1:1 mineral. The XRD traces (Fig. 5) clearly showed a small amount of an expandable mineral with a high K content which could be an illite-smectite. Very weak TEM microdiffraction effects near 4·6, 2·74 and 2·54 Å confirm this interpretation, and in addition provide evidence for the presence of such a mineral in the spherical habit of halloysite. IR spectroscopy, showing the persistence at 180°C of a broad band between 3450 and 3600 cm^{-1} and the shoulder near 880 cm^{-1} on the 910 cm^{-1} band of halloysite, suggests the presence of a poorly crystallized Fe-rich 2:1 clay mineral. From TGA, a theoretical mixture of ~74% halloysite and 26% 2:1 clay mineral is indicated, enabling calculation of the approximate chemical composition of the hypothetical 2:1 clay mineral, assuming that the allophane content is <1%.

The problem is whether there is a mixture of discrete phases or an interstratification of the clays. Several data point to an irregular interstratification of halloysite and illite-smectite: (i) the XRD patterns (Fig. 5a′, b, c, d) show that there is not a mixture of two well crystallized 1:1 and 2:1 clay minerals, but there are some interferences between the reflections of the two components (after the observations made by Cradwick & Wilson, 1972, and Herbillon *et al.*, 1981); (ii) the TEM data confirm this at the scale of the spherical particle (doublets of *hk* reflections near 4·6–4·44 Å, 1·74–1·69 Å, 1·54–1·485 Å); (iii) the IR spectra do not show any distinct band of a well crystallized ferriferous 2:1 clay.

Nevertheless, the presence of some crumpled lamellar clays, like beidellite forms, as well as very few mica particles, could point to a mixture, but some Fe-rich halloysites have a similar crumpled lamellar shape (Tazaki, 1982; Quantin *et al.*, 1984). In addition, Tazaki (1982), showed by *in situ* STEM analysis of several forms of halloysite of various origins that the lamellar forms, as well as the spherical ones, are often rich in Fe and silica. Churchman & Theng (1984) confirmed that non-tubular forms of halloysite are rich in Fe.

The high contents of Fe and Ti could be explained by the presence of very fine particles of Ti-magnetite. Some small (diameter $\simeq 10^{-1}$ nm) opaque discs were detected by TEM at the surface or between the bands of spherical clay particles. The Fe_2O_3/TiO_2 ratio of the whole clay is twice as low as in Ti-magnetite and so some of the Fe and Ti oxides could be present in the 2:1 clay structure, as is the case for some illites and illites-smectites (Weaver & Pollard, 1973).

Imbert & Desprairies (1987) observed in thin section the successive formation in close proximity to each other (0·1–0·2 μm) of Fe-rich illite and spherical halloysite from the weathering of rhyolitic glass in sea water. This could suggest a process for the formation of the Fe-rich halloysite and indeed, this kind of clay occurs at an early stage in the weathering of volcanic glass when the environment is rich in silica, bases, Fe and, possibly, Ti (Tazaki, 1982; Wada & Mizota, 1982; Wada & Kakuto, 1985; Quantin *et al.*, 1984; Quantin & Rambaud, 1987). Thomassin *et al.* (1985) showed the direct formation of Fe-rich smectites at

the expense of basaltic glass, as a result of the *in situ* concentration of Fe and Ti, and Shayan (1984) observed a spherical form of hisingerite derived from the weathering of basalt. Quantin (1985) and Quantin & Rambaud (1987), showed the formation of Fe-rich allophane or hisingerite during the first stage of weathering of basaltic ash in an environment very rich in bases and silica, followed by a transition to an Fe-rich spherical halloysite. In addition, Delvaux *et al.* (1987) observed that similar clays show a selective K^+ adsorption, which can be explained by the interstratification of some smectite in the spherical halloysite. This could be similar to the halloysitic clay studied as it is derived from a trachytic glass, very rich in K.

The preceding data lead us to suggest the hypothesis of an irregular interstratification of halloysite and illite-smectite, in the proportion of ~74% theoretical halloysite, and 26% 2:1 clay. The approximate composition of the unknown 2:1 clay can be calculated from the whole composition of an elementary grain of clay (*in situ* microprobe analysis, Table 2), by subtracting the equivalent proportion of SiO_2 and Al_2O_3 for 74% of theoretical halloysite, and some impurities (TiO_2 and Fe_2O_3 in ilmenite, CaO and P_2O_5 in apatite, and SO_3). Neglecting traces of allophane and Al, Fe hydroxides, this yields the following analysis (normalised in % of anhydrous clay): 42·75% SiO_2, 19·11% Al_2O_3, 26·7% Fe_2O_3, 1·29% MgO, 1·72% CaO, 7·2% K_2O and 1·21% Na_2O. Assuming 8 cations (Si, Al) in the tetrahedral sheet, and 4 cations (Al, Fe, Mg) in the octahedral sheet, the structural formula is $(Si_{5\cdot88}\ Al_{2\cdot12})$ $(Al_{0\cdot98}\ Fe^{3+}_{2\cdot76}\ Mg_{0\cdot26})\ O_{20}(OH)_4\ Ca_{0\cdot26}\ K_{1\cdot26}\ Na_{0\cdot32}$.

This formula is hypothetical and represents an Fe-rich dioctahedral 2:1 clay mineral, with a high negative charge of tetrahedral origin, and so is related to vermiculites rather than smectites. This hypothetical result is analogous to the previous interpretation of the Fe-rich white "halloysite" from Vate (Quantin *et al.*, 1984). The high tetrahedral charges balance the sum of exchangeable cations fairly well. The high K^+ content originates from the weathering of the trachytic glass. But the real structure of this ferriferous 2:1 clay has not been solved. Is it an Fe-rich illite-vermiculite? How can this mineral be associated with halloysite in the same spherical habit? More detailed study is required.

CONCLUSIONS

The weathering of trachytic pumice can directly produce 10 Å halloysite in the waterlogged environment of pyroclastic tuff. Glass is replaced by clay without change in the original fibrous texture, and the *in situ* clay composition is almost homogeneous on the scale of an elementary grain (1 μm^3). The white halloysitic clay is mostly spherical, is rich in Fe and K, and its chemical and mineralogical properties suggest that it is an interstratification of ~74% halloysite and 26% 2:1 clay mineral, the content of allophane and non-crystalline oxides being 1% at most. The calculated formula of the hypothetical 2:1 clay shows that it is a very ferriferous mineral, with high tetrahedral substitution and high K content suggesting that it is more related to vermiculite than to beidellite. Consequently the complex halloysitic clay could be an interstratification of halloysite with an Fe-rich illite-vermiculite mineral, but this hypothesis needs to be verified by the *in situ* study of spherical forms of the clay.

ACKNOWLEDGMENTS

The authors thank the staff of the ORSTOM Laboratories of Mineralogy and Petrology for their contributions to the analyses of the weathered pumice, namely: Mrs A. Bouleau for TEM and microdiffraction, Mrs G.

Millot & Mrs Y. Lafitte for XRD, IR spectroscopy and thermal analysis, Mrs H. Guenin & Mrs M. Gautheyrou for chemical analysis of the weathered pumice extracts, and M. S. Locati for his help with SEM and microprobe analysis.

REFERENCES

BIDINI D., QUANTIN P., DABIN B., LORENZONI P. & LULLI L. (1987) Studio pedologico dell'apparato vulcanico di Vico; VII—Aspetti genetici dei suoli delle colate piroclastiche. *Ann. Ist. Sper. Studio e Difesa del Suolo, Firenze*, **XVII**, 127–158.

BONATTI S. & GALITELLI P. (1950) Metahalloysite Fe di farine fossili di Bagnoregio (Viterbo). *Atti Soc. Toscana Sci. Nat. Ser. A*, 57–100.

CAILLERE S. & HENIN S. (1963) *La Minéralogie des Argiles*, p. 373. Ed. Masson, Paris.

CHURCHMAN G.J. & THENG B.K.G. (1984) Interactions of halloysites with amides: mineralogical factors affecting complex formation. *Clay Miner.* **19,** 161–175.

CRADWICK P.D. & WILSON M.J. (1972) Calculated X-ray diffraction profiles for interstratified kaolinite-montmorillonite. *Clay Miner.* **9,** 393–406.

DELVAUX B., HERBILLON A.J., DUFEY J. & VIELVOYE L. (1987) Relationships between clay mineralogy and K^+ selectivity in a soil chronosequence on basaltic ash deposits from Cameroon. *Summaries—Proc. 6th Meet. European Clay Groups*, 198.

FARMER V.C. (1974) The layer silicates. Pp. 331–363 in: *The Infrared Spectra of Minerals* (V. C. Farmer, editor). Mineralogical Society, London.

GOODMAN B.A., RUSSELL J.D., FRASER A.R. & WOODHAMS F.W.D. (1976) A Mössbauer and IR spectroscopic study of the structure of nontronite. *Clays Clay Miner.* **24,** 54–59.

HERBILLON A.J., FRANKART R. & VIELVOYE L. (1981) An occurrence of interstratified kaolinite-smectite in a red black toposequence. *Clay Miner.* **16,** 195–201.

IMBERT T. & DESPRAIRIES A. (1987) Neoformation of halloysite on volcanic glass in a marine environment. *Clay Miner.* **22,** 179–185.

KUNZE G.W. & BRADLEY W.E. (1964) Occurrence of a tabular halloysite in a Texas soil. *Clays Clay Miner.* **12,** 523–527.

LENZI G. & MATTIAS P. (1978) Materiali "argillosi" della regione volcanica sabatina 1° argillificazione di formazioni piroclastiche. *Rend. Soc. Ital. Mineral. Petrol.* **34,** 75–99.

LORENZONI P., QUANTIN P., BIDINI D. & LULLI L. (1986) Studio pedologico dell'apparato vulcanico di Vico; VI—Caratteristiche mineralogiche dei suoli delle colate piroclastiche. *Ann. Ist Sper. Studio e Difesa del Suolo, Firenze*, **XVII**, 99–126.

LULLI L., BIDINI D. & QUANTIN P. (1988) Climo and litho-soil-sequence on the Vico Volcano (Italy). *Cah. ORSTOM Sér. Pedol.* **XXIV** (in press).

PARFITT R. & HENMI T. (1982) Comparison of an oxalate-extraction method and an infrared spectroscopic method for determining allophane in soil clays. *Soil Sci. Plant Nutr.* **28,** 183–190.

QUANTIN P. (1982) Proposition du taux de capacité d'echange de cations dépendante du pH, comme critère de classification des Andosols des Nouvelles-Hébrides (Vanuatu). *Cah. ORSTOM, Sér. Pédol.* **XIX,** 369–380.

QUANTIN P., HERBILLON A.J., JANOT C. & SIEFFERMAN G. (1984) L'halloysite blanche riche en fer de Vaté (Vanuatu). Hypothèse d'un édifice interstratifié halloysite-hisingérite. *Clay Miner.* **19,** 629–643.

QUANTIN P. (1985) Presence of iron-rich allophane or hisingerite in an Eutrandept derived from basaltic ash, Aoba, Vanuatu. *Abstracts Int. Clay Conf. Denver*, p. 192.

QUANTIN P. & RAMBAUD D. (1987) Genesis of spherical halloysite from basaltic ash, at Ambrym (Vanuatu) Pp. 505–522 in: *Geochemistry and Mineral Formation at the Earth Surface* (R. Rodriguez Clemente & Y. Tardy, editors). CSIC, Madrid.

SHAYAN A. (1984) Hisingerite material from a basalt quarry near Geelong, Victoria, Australia. *Clays Clay Miner.* **32,** 272–278.

SHOJI S. & MASUI J. (1971) Opaline silica of recent volcanic ash soils in Japan. *J. Soil Sci.* **22,** 101–108.

SOLLEVANTI F. (1983) Geologic, volcanologic, and tectonic setting of the Vico-Cimino area, Italy. *J. Volcanol. Geotherm. Res.* **17,** 203–217.

TAZAKI K. (1982) Analytical electron microscopic studies of halloysite formation processes. Morphology and composition of halloysite. *Proc. Int. Clay Conf. Bologna-Pavia*, 573–584.

THOMASSIN J.H., CROVISIER J.L., TOURAY J.C., JUTEAU T. & BOUTONNAT F. (1985) L'apport de la géochimie expérimentale à la compréhension des interactions eau de mer-verre basaltique entre 3° et 90°C: données de l'analyse ESCA, de la microscopie et de la microdiffraction électronique. *Bull. Soc. Géol.* 8, t.I, **2**, 217–222.

WADA K. & KAKUTO Y. (1985) Embryonic halloysites in Ecuadorian soils derived from volcanic ash. *Soil Sci. Soc. Amer. J.* **49**, 1309–1318.

WADA K. & MIZOTA C. (1982) Iron rich halloysite with crumpled lamellar morphology from Hokkaido, Japan. *Clays Clay Miner.* **30**, 315–317.

WEAVER C.E. & POLLARD L.D. (1973) *The Chemistry of Clay Minerals*, p. 153. Elsevier, Amsterdam.